Localised Galvanic Corrosion Processes in Thermal Spray Coated/Cast Aluminium Alloy systems

D. Culliton[a], A. Betts[b], D. Kennedy[a]

a Dept. Mechanical Engineering, Bolton Street DIT D1, Dublin, Ireland

b Dept. Research and Enterprise, 146-147 Lwr. Rathmines Road D6, Dublin, Ireland

SUMMARY : Cast Aluminium Alloys, because of the propensity of aluminium to react with impurities and alloying elements, are prone to developing IM impurities during the solidification process. These IM phases can act, in some fluids, as initiation sites for localised corrosion processes, resulting in degradation phenomena, such as pitting. Whilst Thermal Spray coatings can improve the wear resistance of Cast Aluminium Alloys, their corrosion performance may be hampered by the presence of through porosity within the coating.

The present work details some preliminary studies of the localised corrosion processes occurring at the interface area between a Thermal Spray coating and a cast aluminium alloy. Using the SVP100 SVET system, cross sections of the coated samples, immersed in a NaCl or NaCl/HCl solution, were scanned, over extended periods, in order to map the progressive development of cathodic and anodic areas. EIS sampling, over periods of up to 72 hours, and the results of the Acidified Salt Spray cabinet testing are also presented.

Although only preliminary work has been performed thus far, the premise that the presence of more noble metals along the path of open pores in Thermal Spray coatings on cast Aluminium Alloy, LM25, in the presence of an aggressive aqueous solution, results in the expedited corrosion of the substrate is demonstrated. This occurs, preferentially, around the intermetallic phases, predominantly Fe-based, and results in further destruction of the coating, through spalling, exposing additional substrate to corrosive attack.

Keywords : Cast Aluminium Alloys, Corrosion, Thermal Spray coatings, SVET, EIS

1. INTRODUCTION

Aluminium, in its natural state, is a highly reactive metal but rapidly forms an oxide layer, which protects the underlying material from further attack. However, the mechanical properties of pure aluminium are poor and have few inherent engineering values. Elements such as Si, Fe, Mg and Cu, can be added to the melt, to improve properties ranging from castability to strength, or can be found in the melt as unwanted impurities. The presence of these elements leads to the formation of intermetallic(IM) phases, which are predominantly formed during solidification, as a result of the low solid solubilities of the impurities. In cast aluminium alloys, such as LM25(heretofore LM25 shall refer to all denotations of the AlSi7Mg alloy, including BS EN AC42300 and A356), along with the additions of Si and Cu, transition metals such as Fe and Mn are always present. During casting of aluminium alloys, these impurities cause the formation of a wide variety of IM phases such as Al_2Cu, AlFeSi and Al_3Fe, Al-Fe and Al-Fe-Mn-Si, which form among the aluminium dendrites with various unit cells and morphologies, including platelet(β) and Chinese script(α). Of these elements, Fe is the most important, due to its effect on the engineering properties of the alloy, which is related to its percent presence and its solid solubility. In equilibrium, iron has a very low solid solubility(0.05 wt%) in aluminium[1] and, during cooling, virtually all of the iron present in the alloy will form IM phases of the Al_mFe form or will combine with other elements, such as Si, to form Al- Fe-M compounds. Owing to this limited solid solubility, the volume fractions of such IM compounds are very limited and they are generally quite coarse (0.5 to 10 μm). In addition, the formation and growth of these IM phases is inextricably linked with the cooling rate[2].

Uncoated Aluminium Alloys are prone to corrosion due to the presence of inhomogeneities, often in the form of IM phases, at the surface. These IM phases, particularly those containing Fe or Cu, can prevent the formation of the protective oxide layer[3] and generally act as "active sites" for corrosion, resulting in the dissolution of the aluminium[4,5,6,7,8] and the formation of a pit. As a result of aluminium depletion, the IM phases become rich in the more noble elements, such as Fe or Cu. Accordingly, these zones become more cathodic and further pit growth occurs. This further prevents the formation of a protective oxide layer on the surface and results in extensive degradation of the system. Though IM phases containing other alloying elements, such as Si and Mg, are not as detrimental to the growth of the oxide layer, the thickness and congenerous nature of the oxide layer is in question on these alloys - it is generally accepted that amorphous structures possess superior corrosion resistance than crystalline structures[9] and the presence of these mixed crystalline/amorphous oxide-layer structure can lead to selective leaching and attack of the oxide layer at areas of high crystallinity, resulting in pitting corrosion.

Pitting corrosion occurs when the aqueous environment contains aggressive anions (chlorides, sulphates or nitrates) and occurs above a certain pitting potential (E_p). This pitting potential depends on the composition of the alloy and the concentration of aggressive species. The mechanism can be divided into two steps:

1. The passive oxide film is dissolved, due to the interaction with the aggressive species. This reaction usually takes place at "active" sites, such as Al_2Cu, α-$AlFeSi$ or Al_3Fe[10] inclusions.

2. The exposed aluminium substrate reacts strongly with the species and creates a pit. The pit develops two distinct zones, and sets up a galvanic cell process where the tip of the pit acts as the anode and the top of the pit is the cathode.

Al and H_2O are converted into ions, Al^{3+} and OH^- respectively, and react together to form an $Al(OH)_3$ deposit (white powder or gel formed locally on the surface of aluminium alloys). Inside the pit, H_2 is produced, which causes further destruction of the protective oxide film at the surface, maintaining a pH within the pit, of about 3.5.

Similar phenomena occur in the presence of nitrates and sulphates but the corrosion rate is much slower. This is attributed to an inhibitive role played by nitrates or sulphates, at high concentrations, when these anions are mixed with chlorides.

Thermal Spray coatings generally afford vastly improved wear properties to aluminium alloys. However, the nature of these high wear-resistant coatings introduces a complication through the presence of through-pores and more noble metals – leading to the selective dissolution of the exposed substrate and, eventually, spalling and degradation of the coating.

As corrosion occurs via electrochemical reactions, electrochemical techniques, such as Electrochemical Impedance Spectroscopy(EIS) and Scanning Vibrating Reference Electrode Technique(SVET), are ideal for the study of corrosion processes[11]. Bulk Corrosion processes can be measured through EIS, where a metal sample with a surface area of a few square centimetres is used to model the metal in a corroding system - the metal sample is immersed in a corrosive solution, with a reference and counter electrode, and all the electrodes are connected to a potentiostat. SVET is used to monitor and measure localised corrosion processes, where anodic and cathodic cells develop over the surface of the exposed material.

2.0 AIMS AND OBJECTIVES

The aims of this study are to

- Analyse the EIS nature of the interactions between Thermal Spray coating/Aluminium Alloy, heretofore called the Hybrid System.
- Study the localised corrosion dynamics of the Hybrid System using the Scanning Vibrating Reference Electrode Technique (SVET)
- Model the Hybrid System in a variety of electrolytes and pH values.
- Develop an understanding of the driving and retarding forces involved in the corrosion of these Hybrid Systems.

3.0   EXPERIMENTAL

3.1 Test Panels

- Test Panels were prepared by gravity casting, produced by Alcast Group(Ireland). The aluminium alloy, LM25, has a high silicon content of 6.5-7.5% and was chosen because it is one of the most prevalent cast alloys used in industry. 90 test panels were cast to give a test area of ~100cm^2.
- Spark Spectroscopy was performed on a random test piece sample, to confirm the alloy composition. This was performed at CMA(TCD, Ireland) on a WAS Foundry Master, which is an Arc-spark Optical Emission Spectrometer.
- Samples were also sectioned, mounted, ground and polished to confirm the microstructure of the cast material.
  - The samples were mounted in a 24 hour cure epoxy resin.
  - Grinding was carried out on an EcoMet® Twin Grinder/Polisher using SiC paper, followed by Diamond Polishing and

then final polishing on 0.05µm paste.
- o Microstructural analysis was performed on a Reichert-Jung Me3 metallurgical microscope combined with PC-based image capturing software.

3.2 Thermal Spray Application

Prior to the coating, the panels were first sand blasted using alumina grit, to remove surface contaminants and provide a key for the Thermal Spray coating. The coatings were then applied using the HVOF Thermal Spray system(Figure I).

3.3 Coating Thickness Measurements

Coating Thicknesses were measured with a Fischerscope, which uses eddy currents to measure the coating thickness on non-ferrous substrates. 5 panels per coating system were tested and measurements were taken at 5 points on each test face. The average reading, for each system, was then calculated and noted as the Coating Thickness. These measurements were confirmed using microscopic analysis of cross-sections.
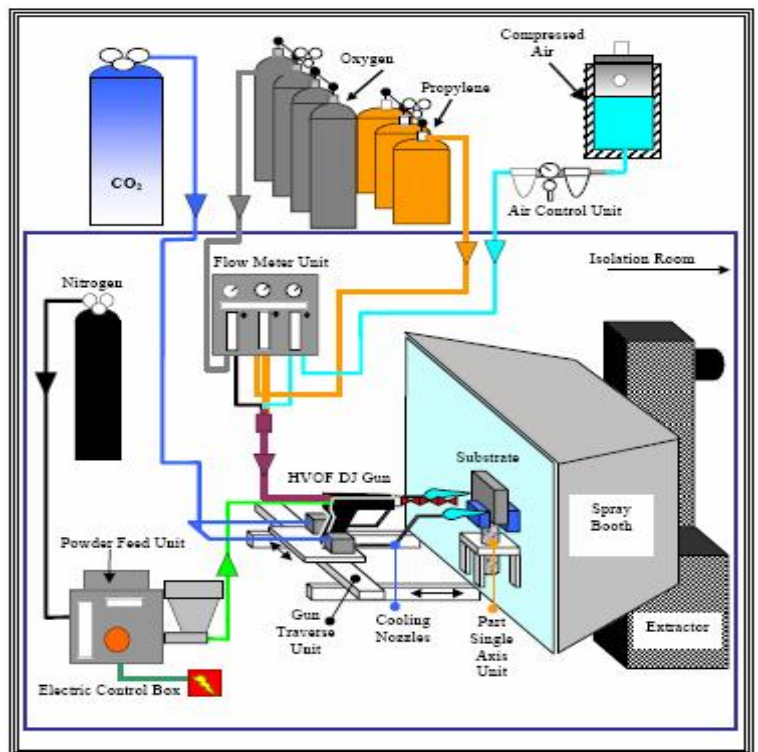

Figure I Thermal Spray (HVOF) application system

3.4 Corrosion Testing

Three 100cm^2 panels were tested for each coating system. All exposed areas outside the test area were sealed by protecting the edges and back of the panels with polyurethane and using insulating tape on the edges for additional protection.

3.4.1 Exposure Cabinet Testing

A minimum of three panels were tested in each environment. The Exposure Cabinet Testing was performed for 6 weeks (1000 hours) in an Acidified Salt Spray(ASS) environment. Table I indicates the details of these tests:

Test	Enviromnent	Temperature / Humidity	Standard
ASS	Acetic Acid + NaCl (pH 3.1-3.3) Ratio: Acetic Acid:NaCl:H$_2$O 10ml:5kg:10L	35°C / 80%RH	EN ISO 3231

Table I The Long Term Corrosion (ASS) Test Environments

3.4.2 Accelerated Testing

3.4.2.1 EIS

EIS is an electrochemical technique that enables the real time behaviour of coatings on metallic alloys to be assessed. The development of various processes, such as diffusion of water through a coating and the onset of corrosion, are progressively reviewing over a period of time, during which the coating is exposed to an environment containing corrosive chemicals - including acids, alkalis and chlorides and/or sulphate species. The electrochemical cell normally used in EIS experiments comprises a three electrode system (Figure II).
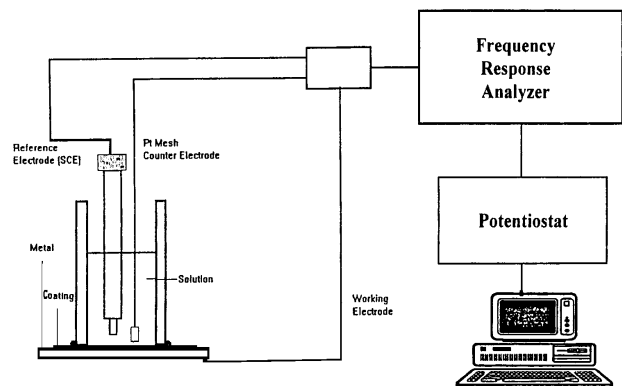

Figure II Schematic of the setup for Electrochemical Impedance Spectroscopy testing.

The preliminary solution, chosen on the basis of the ASS Cabinet Test regime, is as follows:

3

- NaCl+$(NH_4)_2 \cdot SO_4$; pH (near neutral) [Harrison's Solution]

In this preliminary work, EIS was used to measure the Polarisation Resistance of the coated systems, as per the standard ASTM G59, and was performed for 24-120 hours, depending on the performance of the coatings and the solution. When the R_p is known the current density, i_{corr} can be calculated using the following equations :

$$R_p = B/i_{corr} \quad \dots\dots\dots\dots \text{ Eq(1)}$$

where:

- R_p is the polarisation resistance (Ωcm^2)

- i_{corr} the corrosion current ($\mu A cm^{-2}$)

- The proportionality constant , B, for a particular system can be calculated, using the Stern and Geary equation, from b_a and b_c, the slopes of the anodic and cathodic Tafel slopes(Figure v), ie $B = b_a b_c/(2.303(b_a+b_c))$

Once i_{corr} has been calculated, the Corrosion Rate for the experiment can be determined. For aluminium alloys, however, this is a much more complex analytical operation, as the corrosion processes of these systems are predominated by pitting corrosion and, therefore, standard equations cannot be applied.

3.4.2.2 SVET

In aluminium alloys, corrosion is a highly localised process. General corrosion measurement techniques can quantify bulk process parameters but localised galvanic processes require a dynamic measurement technique, such as either the Scanning Resistance Electrode Technique(SRET) or SVET. Representation of the functionality of SVET system is displayed in Figure III[12]. SVET, a development of SRET, provides a lower detection limit and higher resolution and, under controlled conditions, can be used to indicate the evolution of pitting with time[13]. Instead of the dual probe arrangement used in SRET, SVET incorporates a solitary electrode which vibrates perpendicular to the surface, using a piezoelectric vibrator. The potential distribution within the electrolyte above the surface (30-100µm) is measured using a single
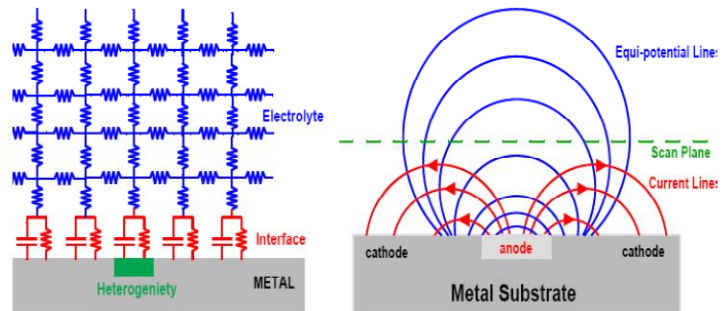

Figure III Illustration of a resistance model for a reactive surface in an electrolyte and the equivalent equi-potential lines.

electrode vibrating between two points and the potential is recorded at the highest and lowest probe position, resulting in a sinusoidal AC signal. Signal processing is performed using a lock-in amplifier and a differential electrometer. The lock-in amplifier, set to the frequency of vibration, clears the signal by filtering out noise from all other frequencies. The detection limit and resolution is improved considerably by using a vibrating probe instead of a stationary dual probe. Probe vibration amplitudes, typically 1µm to100µm, decreases the magnitude signal observed with respect to the SRET, but due to an increased signal to noise ratio achievable by use of a lock-in amplifier and signal averaging, low current measurements in a minimal time can be achieved with a detection limit, for the SVP100, to be below 5µA/cm^2.

For these experiments, two solutions were used: 0.05M NaCl was used for testing the Inconel 625 samples and a 0.05M NaCl/0.008M HCl solution was used for testing the SS317L samples.

3.4.3 Visual Analysis

The Exposure Cabinet tests were reviewed on a daily basis to detect and note surface changes.

3.4.4 Microstructural Analysis

A selection of each coating and Cabinet Test Environment were sectioned using a Milling Machine. Two 15mm^2 samples were taken from each selected panel. Samples were then carefully mounted in Buehlers Epomet F resin.

Polishing and Grinding were performed on the mounted samples using a Buehler system. Due to the complexities involved in producing high-quality micrograph specimens of a soft substrate coated with a hard coating, a substantial amount of time was spent working on the combinations of SiC grinding and Diamond polishing grades. Table II indicates the system that was followed. The samples were thoroughly cleaned with distilled water between each step.

Step			Time(min)
1		240 Grit	3.5
2	SiC Paper	600 Grit	3.5
3		900 Grit	3.5
4		1200 Grit	3.5
5	Diamond Paste / Microcloth	9 µm	3.0
6		6 µm	3.0
7		3 µm	3.0
8	Final Polishing	0.05 µm	3.0

Table II Grinding and Polishing Steps developed for this project.

3.4.5 Scanning Electron Microscopy

The corrosion product, from a selection of samples, was tested using the Scanning Electron Microscope(SEM), in order to identify the elements present. SEM analysis was performed on a Jeol JXA8600 equipped with a PGT elemental detector.

4.0 RESULTS AND DISCUSSION

4.1 Spark Emission Spectroanalysis

Chemical Analysis was carried out on the cast LM25 alloy using Spark Emission Spectroanalysis. The results, detailed in Table III, show the analysis versus the ISO/BS Standard composition for this alloy.

4.2 Coating Thickness

The stipulation on coating thickness was 100µm maximum. Coating thickness measurements of the HVOF coatings are approximately 100µm, as detailed in the Table IV.

4.3 Exposure Cabinet Testing

The application of a coating aims to provide a protective layer on the surface and prevent attack by aggressive complexants, such as chloride and sulphate. In this investigation, an SS316L panel was included, to act as a benchmark system, against which the performances of the Thermal Spray coating systems were measured. It is evident from the results that the unsealed systems provide no protection against corrosion attack in any of the exposure environments. The Exposure Cabinet testing was performed up to a maximum period of 1000 hours(ASS).

Element		Analysis	LM25 Specification
Si		6.924	6.5 – 7.5
Fe		0.285	0.55 (0.45)
Cu		0.092	0.20 (0.15)
Mn		0.195	0.35
Mg		0.268	0.20 to 0.65
Ni		0.007	0.15
Zn		0.077	0.15
Pb		0.006	0.15
Sn		0.010	0.05
Ti		0.087	0.15
Others	Each	-	0.08
	Total	-	0.10
Al		Remainder	Remainder

Table III Spark Emission Spectroanalysis results of the cast Al-alloy.

4.3.1 Acidified Salt Spray (1000 Hours)

Figure IV show the test panels from the Acidified Salt Spray Test. Each set were tested for a full 1000 hours and the purpose of this test was to expose the coating systems to a high-humidity, chloride environment. However, the photographs were taken at the point of failure of the coating systems. The Inconel 625 and SS317L panels showed degradation after only 24 hours of exposure- Figure IV(a,b). The corrosion product appeared as blistering over the exposed surface.

Application	Coating	Average Thickness (mm)
HVOF	Inconel 625	105
	SS317L	100

Table IV Thermal Spray Coating Thickness measurements

Figure IV(c) shows the 316L panels after 1000 hours exposure. It can be seen that no degradation of the surface occurred on these panels.

The presence of high levels of chloride has been shown to cause extensive pitting in aluminium alloys[14,15,16], particularly around IM phases. This can initiate by the accumulation of Cl$^-$ ions on the metal surface, which cause the dissolution of the oxide layer and exposure of the metal to reducing agents, such as oxygen. This, then, sets up a galvanic cell between the tip and the mouth of the pit. Ordinarily, the pit locations would predominate around areas where the oxide layer was ineffective, such as around IM phases. On these coated samples, the corrosion initiated in areas where open-pores existed in the coating and progressed around the IM phases. It may be surmised that the coatings played an active part in the corrosion process. These coatings were not, however, actively broken down, as SEM analysis of the corrosion product indicated the presence of aluminium and oxygen only, presumably in the form $Al(OH)_3$. XRD analysis proved inconclusive, when attempts were made to analyse the corrosion products. Suggestions that the presence of Mg, in the form of IM phases, in these alloys, would have

resulted in the formation of $Mg(OH)_3$ proved to be unsubstantiable and the undetectability of this element in the corrosion product analysed is taken as further proof that the corrosion processes were driven, primarily, by the Thermal Spray coatings, through open pores in the coating structures and, subsequently, by degradation of the coating.

(a)	HVOF – SS317L 96 hours exposure Extensive Corrosion product apparent after 24 hours.
(b)	HVOF – Inconel 625 96 hours exposure Extensive Corrosion product apparent after 24 hours.
(c)	316L 1000 hours exposure No change to the surface morphology was noted.

Figure IV Test Panels after exposure in the Acidified Salt Spray test

4.4 Microstructural Analysis

All micrographs are of un-etched structures.

4.4.1 Substrate

Aluminium-Silicon cast alloys usually contain impurities, such as Fe, that form hard IMs with high melting point and with various morphologies, including platelet (β-AlFeSi), Chinese script (α-AlFeSi) and polyhedral (sludge)[17]. In analyses of Al-Si alloys, other investigators[18] have reported the "Chinese-script" morphology to be consistent with a description of body-centred
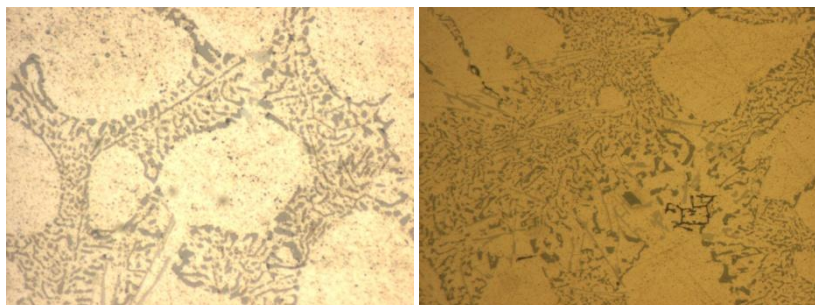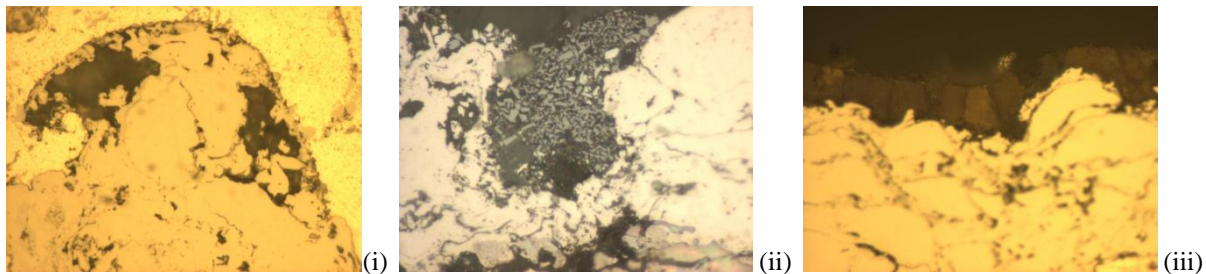

Figure V Photomicrographs showing typical microstructure of LM25/A356 Al-Si Alloy (mag. x500).

cubic $α-Al_{19}Fe_4MnSi_2$ and that the plate-shaped phase is consistent with tetragonal $δ-Al_3FeSi_2$. The platelet, β-, phase is detrimental to the mechanical properties of the alloy and Mn is widely used as an alloying addition to neutralize the effect of

6

iron and modify this phase to less harmful morphologies. Typical microstructures of the LM25 alloy under investigation are shown in Figure V, exhibiting this Chinese Script structure, with the dendritic aluminium grain growth dispersed within a eutectic Al-Si structure. Process-related porosity was not noted on any of the samples viewed.

4.4.2 Coatings

It is widely published[19] that chloride ions have a detrimental effect on the corrosion resistance of aluminium and its alloys and increased levels of Cl⁻ tends to shifted both the pitting potential, E_{pit}, and corrosion potential, E_{cor}, to more active values; thus

Figure VI Cross section photomicrographs showing the degradation of the SS317L HVOF coating in the ASS environment.(i) x500, (ii) x200; (iii) x200

increasing the corrosion rate. On the Inconel 625 and SS317L coatings, corrosion was noted after only 24 hours. Figure VI shows the degradation of the SS317L coating system after exposure in the ASS environment. The dissolution of the alloy beneath the coating, by Pitting Corrosion, Figure VI(i,ii), and the subsequent growth of the oxide layer, Figure VI(iii), resulted in spalling of the protective coating, as shown. This pitting is caused by breaches in the coating as a result of through-pores, which are a generic problem with Thermal Spray coatings. This is followed by the accumulation of Cl⁻ ions at the surface and this accumulation actively breaks-down the oxide layer and prevents growth of a new oxide layer. Once the oxide layer has broken down, corrosion of the substrate proceeds by the dissolution of the aluminium matrix Fe-containing phases, as these phases are cathodic to the surrounding matrix. Similar effects can be seen for the Inconel 625 in Figure VII.
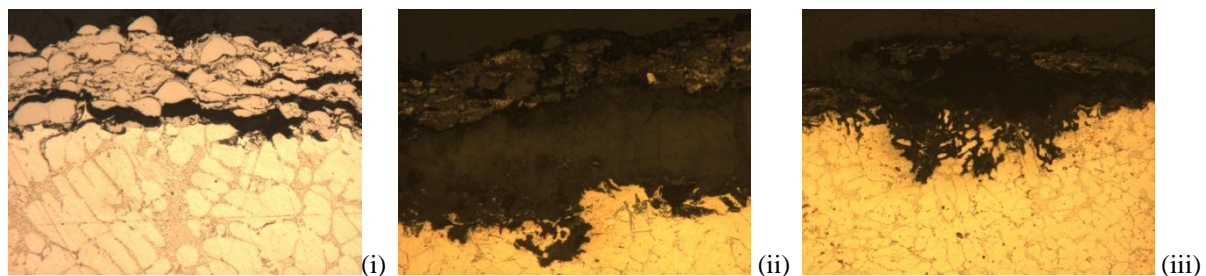
Figure VII Cross section photomicrographs showing the degradation of the Inconel 625 HVOF coating in the ASS environment. (Mag. x200)

4.5 Electrochemical Impedance Spectroscopy Analysis(EIS)

EIS is a non-destructive method of analysis, which assists in the development of predictive life-to-failure theories for systems exposed to corrosive environments. The EIS work performed thus far has been utilised to predict the response of the different systems when exposed to the standard Harrisons Solution(3.5 g/l $(NH_4)_2SO_4$, 0.5 g/l NaCl). For comparative analysis, an untreated panel was chosen as a 'standard' and a passivated 316L panel was chosen as a benchmark; all tests were analysed with respect to these. The mechanism of corrosion of a system depends on the metallic substrate, the composition of its passive layer and corrosion products, as well as on transport phenomena, whilst the microstructure also has an impact. Due to the nature of their surface and sub-surface microstructures, eg the presence of IM phases, aluminium alloys tend to form inhomogeneous oxide layers causing these systems to have diminished corrosion resistance when compared to the pure metal. Figure VIII shows the EIS results of the untreated Al-alloy test panel. It can be noted that whilst the initial Polarization Resistance (R_p) value is low(3×10^2 Ωcm^2) when compared to more resistant systems such as 316L(Figure IX), the reduction over time is minimal (1.5×10^2 Ωcm^2 after 54 hrs). This is typical of aluminium alloys, where the corrosion processes are progressive but do not vary greatly with respect to time as the corrosion product adheres to the surface, creating a barrier against further corrosion. If we now introduce a secondary system, such as a coating, we note that the corrosion process becomes accelerated.

Thermal Spray coatings contain high levels of porosity (2-8%), some of which expose the coated substrate (through-pores) to the surrounding environment. In experimental work performed thus far, the cabinet testing carried out on the coated systems

suggested that, due to the presence of these pores, these Thermal Spray coatings do not provide sufficient corrosion protection to the substrate material. Although not quantified in the work performed to-date, it may be surmised that thinner Thermal
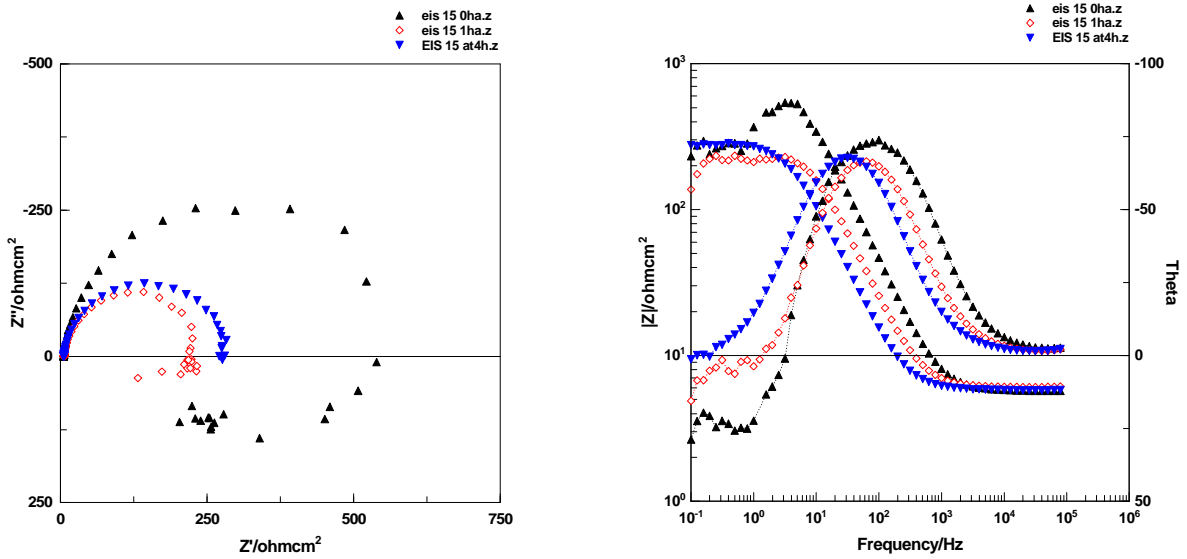

Figure VIII EIS results for an LM25 panel (0, 1 & 4 hrs) in Harrisons Solution, showing the Nyquist(left) and Bode(right) plots.

Spray coatings will result in a higher percentage volume of through-pores, thus exposing more of the substrate to the corrosive environment. In addition, when these porous coatings, containing metals lower on the electrochemical series, are applied to Spray coatings will result in a higher percentage volume of through-pores, thus exposing more of the substrate to the corrosive environment. In addition, when these porous coatings, containing metals lower on the electrochemical series, are applied to the substrate, it can be predicted that the corrosion rate of the exposed substrate will increase, due to the presence of large cathodic areas, provided by the coatings. This configuration leads to a pit-like structure over the surface of the system, with
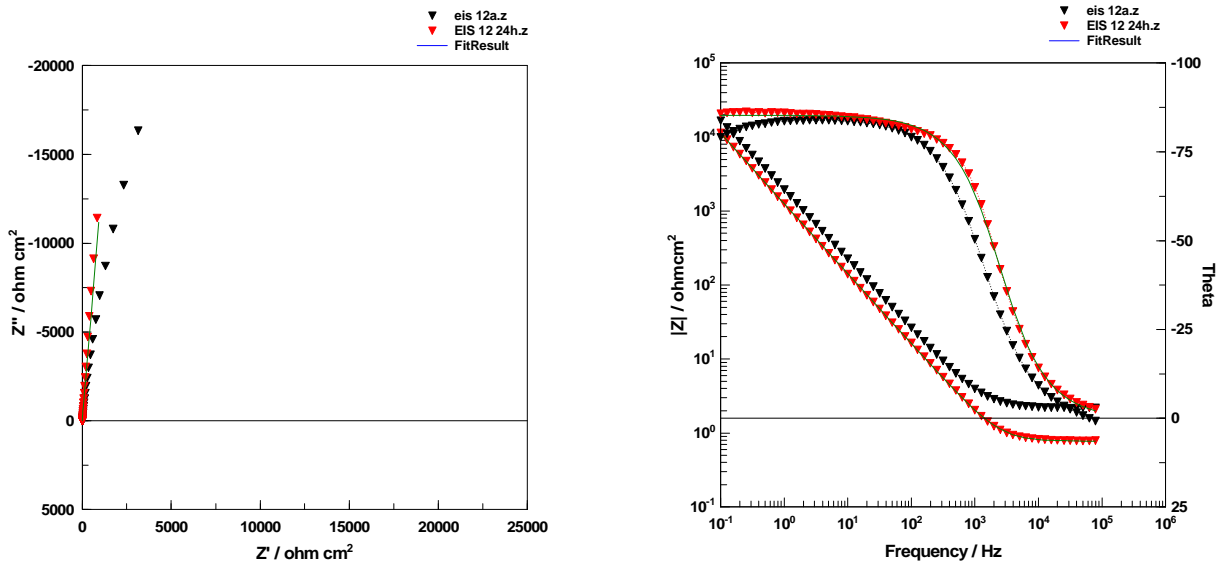

Figure IX EIS results for passivated 316L panel (0 & 24 hrs) in Harrisons Solution, showing the Nyquist(left) and Bode(right) plots.

the cathodic areas provided by the coating, and the anodic tip provided by the substrate. The accelerated corrosion process that ensues is further compounded by the production of the voluminous corrosion product, preventing a retardation of the cathodic reaction. In Figure X and Figure XI we can see that the results of this effect. Figure X shows the EIS results of the SS317L coating. It can be seen that the initial R_p is approximately equal to that of the uncoated panel(2×10^2 Ωcm^2). However, this value drops dramatically over the life of the test(0.2×10^2 Ωcm^2 after 24 hrs). The presence of the more cathodic Ni and Cr create large cathodic areas to the highly anodic Al substrate. In Inconel 625, the high levels of Ni and Fe provide the cathodic impetus for these aggressive corrosion processes. Figure XI gives the results of the Inconel 625 coating, over periods of 0 to 30 hrs, showing similar reductions in the R_p value[2×10^2 Ωcm^2 @ 0 hrs to 1×10^2 Ωcm^2 at 30 hrs]. It can be seen that there is a slight increase in the R_p value between 2 hrs and 30 hrs. This is attributed to the corrosion product acting as a barrier to the corrosive electrolyte. The physical manifestation of these corrosion processes are demonstrated in Figure IV(a)[SS317L] and
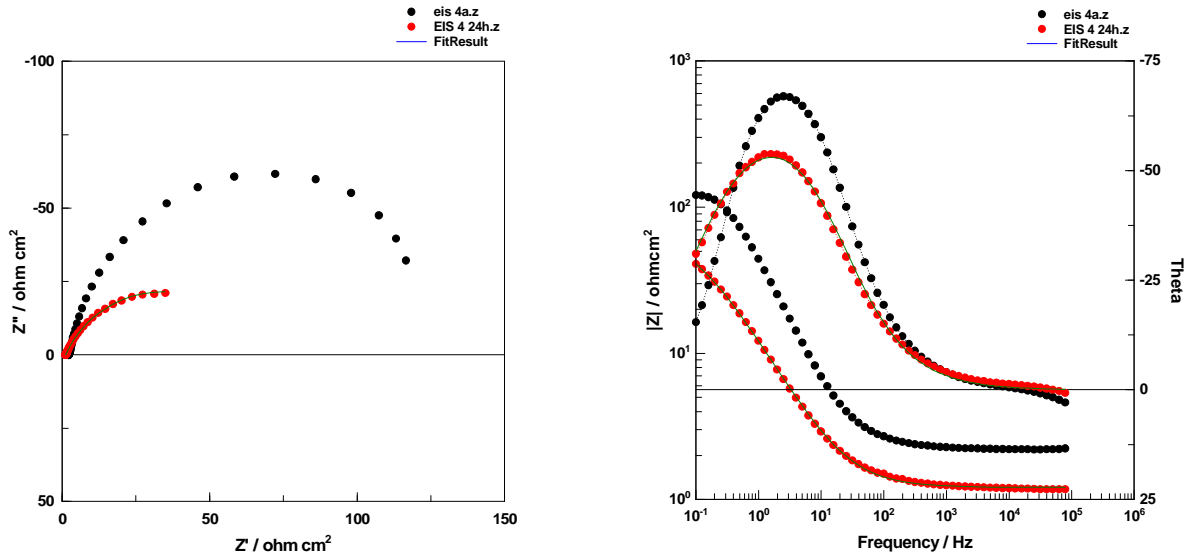
Figure IV(b)[Inconel 625].

Figure X EIS results for SS317L(HVOF) coating (0, 2, 4, 6 & 30 hrs) in Harrisons Solution, showing the Nyquist(left) and Bode(right) plots.

One method of improving the protective nature of these coatings is to incorporate materials that are inert to the substrate. Table V outlines the polarisation resistance values estimated from Bode plots of Frequency versus Impedance magnitude at 100mHz (the lower limit of the scanned frequency range). Due to the low values achieved, indicating a low resistance to
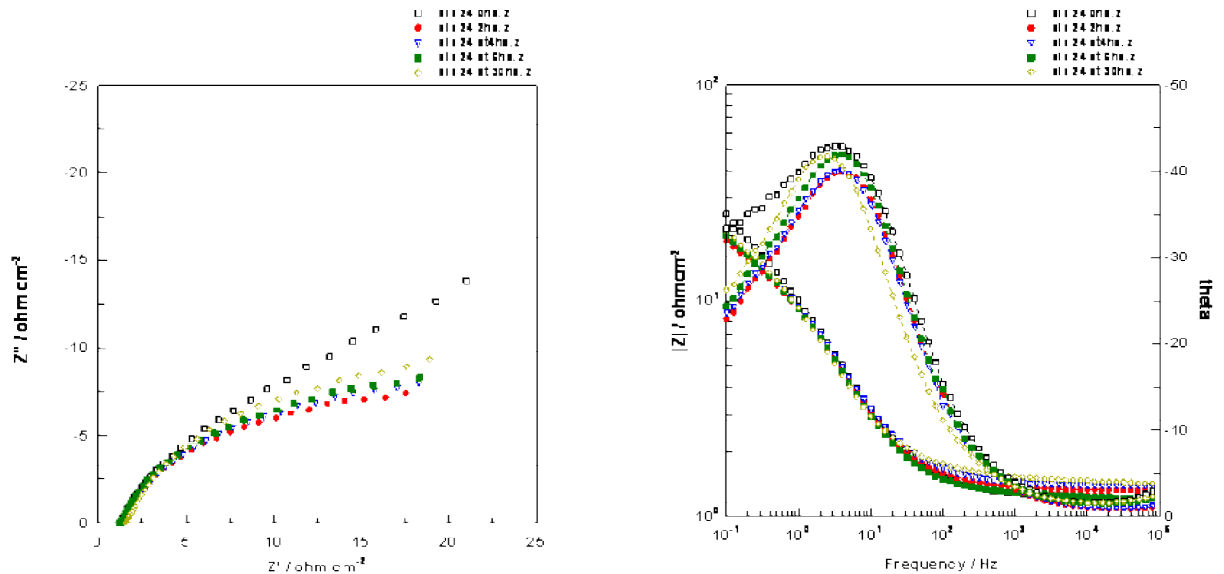

Figure XI EIS results for Inc.625(HVOF) coating (0, 2, 4, 6 & 30 hrs) in Harrisons Solution, showing the Nyquist(left) and Bode(right) plots.

corrosion, it was deemed unnecessary to progress the testing beyond the initial 24 hour period. It may be noted, however, that the rapid degradation of the systems in the ASS are paralleled well by the results of the EIS testing.

	R_{100} / Ωcm^2				
Exposure Time(hours)	0	2	4	8	24
Coating					
Inconel 625 (HVOF)	>7.8 x 10^4	>7.8 x10^2	>1.9 x 10^2	>1.2 x 10^2	
SS317L (HVOF)	1.2x 10^2				
Stainless Steel 12	>1.7 x 10^4	>1.4 x 10^4	>1.1 x 10^4	>1.1 x 10^4	1.1x 10^4

Table V EIS Results in Acidified Harrisons Solution showing Polarisation Resistance values.

The most effective protection system currently available to engineers is a Chromate Conversion pre-treatment over-coated with

paint. Typical R_p values for these coating systems would be about 10^8. As can be seen from Table V, the tested coatings have initial R_p values much lower than this. The subsequent rapid deterioration of these systems is mirrored by the ASS Cabinet Exposure testing results(Figure IV).

4.6 SVET

The results of the SVET testing are shown in Figure XII. Although the results are preliminary results, development of the cathodic and anodic areas are very apparent in the SS317L samples exposed to the NaCl/HCl solution. Over the period of the SS317L test the development of cathodic(blue) and anodic(red) areas around the coating / substrate interface is apparent. It can be seen in the latter scans that these areas not only develop but that the zones also move and disappear from the scan area. It has been reported by Akid et al[20] that the tendency for aluminium alloys to experience pitting corrosion cannot be measured easily by the standard SVET test. It is because of the tendency of the anodic and cathodic reactions to constantly move over the exposed surface areas that this is the case. It can be seen in the SS317L scans that the rate of growth of the cathodic and anodic areas correlates with the performance of the panels in the ASS environment, where corrosion product was noted on the

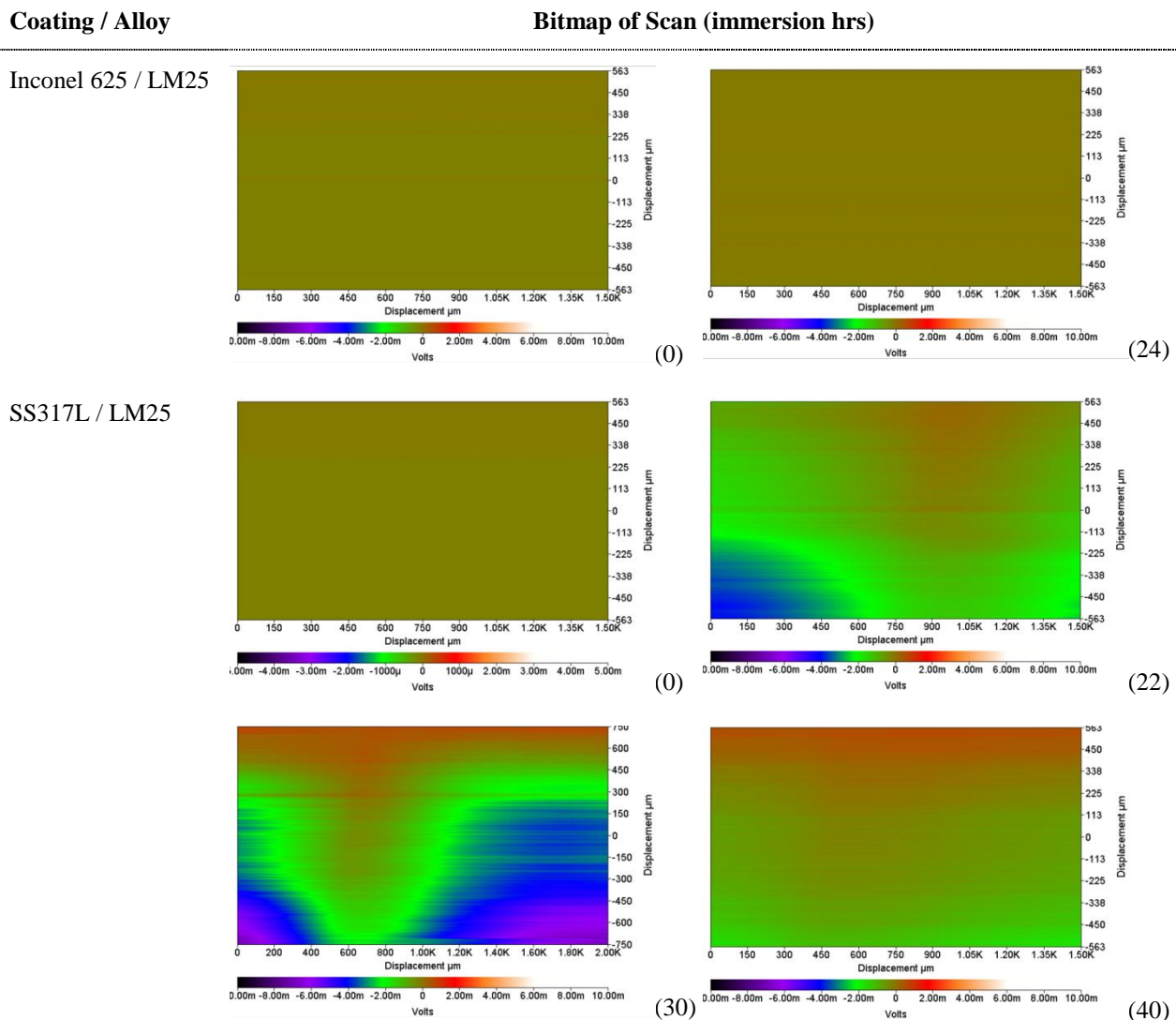| Coating / Alloy	Bitmap of Scan (immersion hrs)	
Inconel 625 / LM25	(0)	(24)
SS317L / LM25	(0)	(22)
	(30)	(40)

Figure XII Showing preliminary SVET Scans for Inconel 625 in 0.05M NaCl and SS317L in 0.05M NaCl/0.004MHCl.

panels within 24 hours of initial exposure. It is suggested, from the results of the EIS and cabinet testing that the corrosion of these hybrid systems is driven by the presence of more noble elements in the coating. The presence of through-pores exposes the substrate to Cl⁻ ions and creates a galvanic cell between the anodic substrate and the cathodic coating. These preliminary SVET scans would suggest that there is a strong tendency of these systems to form these galvanic systems but that the growth of corrosion product may have short-term benefits by restricting the limiting access to either the cathodic or anodic elements. From the 40 hour scan above it can be seen that, though the coating in this area is no longer acting as a cathodic element, there is still strong anodic activity at the substrate.

5. CONCLUSIONS

From the work presented here it may be stated that

1. The hybrid systems perform poorly when exposed to the ASS environment. This poor performance is due to coating/substrate galvanic effects, through porosity and the presence of chloride ions on the stability of the oxide layer.
2. Metallographic inspection showed delamination of the coating at areas of corrosive attack. The growth of the corrosion product at the substrate/coating interface resulted in further spalling and degradation of the coating, further exposing the unprotected substrate to attack.
3. Corrosion products obtained from the cabinet tests were analysed and were found to contain only aluminium and oxygen. This is further proof that the corrosion processes occurring are driven through the pores by the cathodic nature of the coatings
4. Results from the long-term cabinet testing, ASS, correlated well with the short-term tests, EIS. Indications from the EIS results were mirrored by the performance of the hybrid systems in the ASS test.
5. Preliminary results obtained from the SVP100 (SVET) analysis showed the development and movement of separate anode/cathode areas. These developments occurred within 20 hours of exposure to the corrosive environment, which correlates well with the performance observed in both the ASS test and the EIS.

6. FURTHER WORK

1. Further work will be performed in the area of coating of the Test Panels. Additional materials will be applied, including nanostructured powders.
2. The large discrepancy in the ratio between the exposed anodic and cathodic areas are a concern for the SVET analysis. Future work will look at altering this ratio, through masking, to measure the response of the resultant systems.
3. To investigate sealing technologies and their effect on the performance of these hybrid systems.

7. REFERENCES

[1] H. Jones, Journal of Materials Science, 41, pp.6069-6071 (2006)

[2] Małgorzata Warmuzek, Wiktoria Ratuszek and Grażyna Sęk-Sas; Materials Characterization, 54, pp31-40 (2005)

[3] Andrzej S. Nowotnik, Grazyna E. Mrowka-Nowotnik, www.science24.com (accessed November 2007)

[4] P. Campestrini, E. P.M. van Westing, H.W. van Rooijen and J.H.W. de Wit, Corrosion Science, 42, pp1853 (2000)

[5] T. Dimogerontakis, L. Kompotiatis and I. Kaplanoglou, Corrosion Science, 40, pp1939 (1998)

[6] V. Guillaumin and G. Mankowski, Corrosion Science, 41, pp421 (1998)

[7] J.D. Gorman, S.T. Johnson, P.N. Johnson, P.J.K. Paterson and A.E. Hughes, Corrosion Science, 38, pp 1977 (1996)

[8] P. Schmutz and G.S. Frankel, J. Electrochemical Society, 145, pp2295 (1998)

[9] S. Hiromoto, A. -P. Tsai, M. Sumita and T. Hanawa, Corrosion Science, 42, pp2167-2185 (2000)

[10] M. V. Kral, P. N. H. Nakashima & D. R. G. Mitchell, 37, 2006, pp1987-1997

[11] B. Vuillemin, X. Philippe, R. Oltra, V. Vignal, L. Coudreuse, L. Dufour, E. Finot, Corrosion Science 45, 1143–1159 (2003)

[12] J. Gustavsson, University of Woolongong, PhD Thesis 2006

[13] A.M. Simões, D. Battocchi, D.E. Tallman, G.P. Bierwagen, Corrosion Science 49, 3838–3849 (2007)

[14] J. M. Costa, H. Vidal; M. Vilarrasa, Key Engineering Materials, 20-28, pp113-120 (1987)

[15] E.E. Ebenso, P.C. Okafor, U.J. Ekpe, O. Ogbobe, Journal of Applied Polymer Science, 103, pp2810-2816 (2007)

[16] V. Guillaumin, G. Mankowski; Corrosion Science ; 42, pp105-125 (2000)

[17] P. Ashtari, H. Tezuka, T. Sato, Materials Forum; 28, pp951-955 (2004)

[18] M.V. Kral; Materials Letters, 59, pp2271-2276 (2005)

[19] B. Zaid, D. Saidi, A. Benzaid, S. Hadji, Corrosion Science, 50, Pages 1841-1847 (2008)

[20] R. Akid, M. Garmab, Electrochimica Acta, <u>49</u>, pp2871–2879 (2004)